Islamic Azad University

Journal of

Optoelectronical Nanostructures

Winter 2019 / Vol. 4, No. 1

Enhancement of the Magneto-Optical Kerr Effect in One-Dimensional Magnetophotonic Crystals with Adjustable Spatial Configuration

Tahmineh Jalali[*,1], Abdolrasoul Gharaati[2], Mohammad Rastegar[2], Mohammad Ghanaatian[2]

[1] Physics Department, Persian Gulf University, Bushehr, Iran
[2] Physics Department, Payame Noor University, Tehran, Iran

(Received 13 Dec. 2018; Revised 25 Jan. 2019; Accepted 18 Feb. 2019; Published 15 Mar. 2019)

Abstract: We studied magnetophotonic crystals (MPCs) with introduced magnetic defect layer sandwiched between magnetic and dielectric Bragg mirrors. These magnetophotonic crystals have excellent capabilities to enhance reflection and Kerr rotation simultaneously. By adjusting spatial configuration such as repetition numbers of Bragg mirrors and thickness of magnetic defect layer, we achieved the Kerr rotation angles more than 75° and reflection very close to 1. We briefly described the formulation of finite element method (FEM) and transfer matrix method (TMM). The electric field distribution and magnitude of it along the MPCs are simulated using FEM. Using the TMM, we calculated the MO responses of MPCs. With light localization inside the magnetic defect layer and multiple reflections in it, the magneto-optical (MO) responses of these MPCs were significantly increased. The studied structures in this research have high MO responses that make it suitable for designing MO elements in highly sensitive devices and optical telecommunication tools.

Keywords: Magneto-Optics, Magnetophotonic Crystals, Reflectance, Kerr Rotation, Defect Layer

1. INTRODUCTION

Within the past two decades, studying and creating microstructures and nanostructures with high accuracy for using in optical elements and telecommunications has been the subject of intense interest among the researchers. Photonic crystals (PCs) are periodic structures of optical materials with refractive index modulation in one, two, and three dimensions. These structures control and manipulate the propagation of light [1-4]. Initially, one-

*Corresponding author. Email: **Jalali@pgu.ac.ir**

dimensional PCs were introduced by Yablonovitch [5] and John [6]. The propagation of light in the PCs is prevented for some frequency and wavelength regions, which are called Photonic Band Gaps (PBG). The PCs may show localization or guiding of light by introducing the point and line defects in their periodic arrangement. This property is one of the fundamental principles of designing PC devices [3, 7-11]. Magnetism is an important subject of researches in condensed matter physics with many theoretical and experimental measurements of MO effects such as Faraday and Kerr rotations. These effects resulted from the interaction of light with magnetically polarized materials [12,13]. The one-dimensional magnetophotonic crystals (MPCs) are constructed when the defect layers and/or the constituent materials of one-dimensional PCs have magneto-optical (MO) features. The MO effects such as Faraday and Kerr rotations in MPCs, can modulate the optical signal via an external magnetic field [14-18]. By light scattering from the magnetic material or MPCs, the angular momentum is transferred to reflected wave, i.e., the Kerr effect, and transmitted wave, i.e., the Faraday effect. As a result, the produced waves lead to the rotation of the polarization plane of the initial linearly polarized wave [19]. In recent years, many researchers have studied the magnetophotonic crystals because of their unique MO properties, important applications and small optical losses. The applications of magnetic materials have high importance in wide fields like astronomy, defense, industry and materials. These magnetic materials are used for handling data of systems such as smart card and magnetic strip scanning [20,21]. With the presence of a magnetic defect layer in MPC, the electromagnetic wave can be localized inside or in the vicinity of the defect layer and the defect modes are appear inside the PBG [22-24]. The multiple reflections of light in the magnetic defect layer, increase the effective length of light. By constructive interference of reflections, the MO responses of MPC are enhanced [25,26]. Despite the MO effects that are caused by light passing through the magnetized structures, some of these effects exhibit themselves by reflecting the incident light from the surface of MO structures. These phenomena are conventionally designated as magneto-optical Kerr effect (MOKE) [27-29]. The MPCs that display the high MOKE, have important capabilities for applying in recording and reading data from the MO discs and probing magnetized areas on the surface of MPCs [29-32]. Therefore, the MPCs with miniaturized dimensions and high Kerr angle are suitable structures to design magnetic field detectors and high-sensitivity MO sensors [24].

Numerical studies show a trade-off between the reflection value from PCs and angle of Kerr rotation; i.e., a large Kerr rotation angle with decreased reflection. Hence, we are looking for MO structures with significant reflections and high values of the Kerr rotation angles. Additionally, to optimize MO devices for practical applications, we should obtain the MPCs with high MO features by adjusting the spatial configuration which is the subject of this research. The remainder of this paper is organized as follows: In Sections 2 and 3, we briefly describe the computational methods used to investigate the MO properties of one-dimensional MPCs. We discuss the formulation of the transfer matrix method (TMM) and principles of finite element method (FEM). The results of the MOKE calculations for MPCs with magnetic and dielectric Bragg mirrors are presented in Section 4. Finally, concluding remarks are presented in Section 5.

2. TRANSFER MATRIX METHOD

The TMM is an efficient method for the analysis of electromagnetic wave propagation through the multilayered optical media, such as PCs. Using this method and solving the Maxwell equations, we can calculate the reflection and transmission spectra of these periodic structures. Considering the continuity of optical field across the boundaries of adjacent layers, the optical properties of the layered structure can be obtained. This computational framework is used to investigate the MO responses of magnetophotonic crystals, such as Faraday and Kerr rotation. When incident light enters from an initial nonmagnetic environment to a magnetized medium with the arbitrary direction of magnetization vector, the permittivity tensor ε_M can be generalized as follows [27]:

$$\varepsilon_M = \begin{pmatrix} \varepsilon_{xx} & -iQm_z & iQm_y \\ iQm_z & \varepsilon_{yy} & -iQm_x \\ -iQm_y & iQm_x & \varepsilon_{zz} \end{pmatrix} \tag{1}$$

where m_x, m_y and m_z are components of the magnetization vector in the direction of main axes of space [27] and Q is MO parameter of the magnetized medium and for the case with $\varepsilon_{xx} = \varepsilon_{yy}$ as

$$Q = i.\frac{\varepsilon_{xy}}{\varepsilon_{xx}} \tag{2}$$

To analyze the electromagnetic wave propagation through any of the layers of the multilayered structures, the Maxwell equations can be written as [33]:

$$\nabla \times E = i\omega\mu_0 H \tag{3}$$

$$\nabla \times H = i\omega D \tag{4}$$

We used of 4×4 transfer matrix method (TMM) to investigate the MO responses of magnetophotonic-layered structures. To establish this method, we consider the relationship between the tangential components of the electric and magnetic fields in each layer and another set of fields as follows [34]:

$$F = AP \tag{5}$$

with

$$F = \begin{pmatrix} E_x \\ E_y \\ H_x \\ H_y \end{pmatrix} \tag{6}$$

$$P = \begin{pmatrix} E_s^i \\ E_p^i \\ E_s^r \\ E_p^r \end{pmatrix} \tag{7}$$

The components of matrix P, used to express the s-polarized and p-polarized components of the electric and magnetic field for incident (i) and reflected (r) waves. A is the 4×4 medium boundary matrix. For the structures with i (incident layer) and f (final layer), we can be written

$$A_i P_i = \prod_{m=1}^{N} (A_m D_m A_m^{-1}) A_f P_f \tag{8}$$

m is layer number and N is the total number of layers. Here D_m is the propagation matrix of m'th layer [35]. The total transfer matrix of the multilayered magnetophotonic structure is obtained as

$$T_{tot} = A_i^{-1} \prod_{m=1}^{N} (A_m D_m A_m^{-1}) A_f \tag{9}$$

By solving Maxwell equations for light reflection from MO structures and using of these equations, the Magneto-Optical Fresnel reflection matrix can be given as follows [28]:

$$R = \begin{pmatrix} r_{pp} & r_{ps} \\ r_{sp} & r_{ss} \end{pmatrix} \tag{10}$$

where r_{ij} is the ratio of the incident j-polarized electric field and reflected i-polarized electric field. For polar configuration, $m_z = 1$ and $m_x = m_y = 0$. We define the Kerr rotation angle (θ_K) and ellipticity (ζ_K) for p-polarized and s-polarized waves in Magneto-Optical structures, as follows [27]:

$$(\theta_K)_{p-polarized} = \mathrm{Re}(\frac{r_{sp}}{r_{pp}}) \tag{11}$$

$$(\theta_K)_{s-polarized} = \mathrm{Re}(\frac{r_{ps}}{r_{ss}}) \tag{12}$$

$$(\zeta_K)_{p-polarized} = \mathrm{Im}(\frac{r_{sp}}{r_{pp}}) \tag{13}$$

$$(\zeta_K)_{s-polarized} = \mathrm{Im}(\frac{r_{ps}}{r_{ss}}) \tag{14}$$

Where Re and Im represent taking the real and imaginary part of complex number. To optimize the magnetophotonic crystals, the signal-to-noise ratio, should be maximized [36]. This can be done by computing of figure of merit (FOM) as

$$FOM = R.((\theta_K)^2 + (\zeta_K)^2) \tag{15}$$

Where R is optical reflection of magnetophotonic structure. For MO data storage systems, the FOM are of particular importance due to the simultaneous dependence of the reflection values, the Kerr angle and the ellipticity.

3. FINITE ELEMENT METHOD

In this method, the simulation and computation were made based on six steps: 1) Dividing the computational space in to finite elements; 2) Introducing the function representing the physical properties of each element; 3) Achieving the equations for each element; 4) Combining the equations in elements and generating the equations system; 5) Applying the boundary conditions on the location of the element node; and 6) Solving the equations system [37].

The FEM formulation includes weighted residual methods and minimum potential energy. The problem was solved by simpler methods such as Euler method by eliminating the differential equations or simplifying them to ordinary equations. The Maxwell equations were solved by considering the boundary conditions and physical properties of the problem. Using this technique, the electromagnetic waves in the optical and photonic systems can be simulated. The optical tools such as waveguides, cavities, and filters can be simulated and examined by FEM. To study the magnetophotonic structure, the wave equation was solved using the periodic boundary conditions:

$$\hat{n} \times (E_1 - E_2) = 0 \tag{16}$$

$$\hat{n} \times (H_1 - H_2) = 0 \tag{17}$$

Also, we have used of scattering boundary conditions as:

$$\hat{n}\times(\nabla\times\vec{E})-ik\hat{n}\times(\vec{E}\times\hat{n})=-\hat{n}\times(\vec{E}_0\times(i\vec{k}(\hat{n}-\hat{k}_{dir}))).\exp(-\hat{k}_{dir}.\vec{r}) \qquad (18)$$

Where E_0 is incident electric field, n is the normal direction and k_{dir} is the incident wave vector. The first step was related to the mesh structure and its conditions. The properties of mesh structure should enhance the accuracy of computations and use less memory. In fact, the balance between these two factors must be established. These simulated electric and magnetic fields were employed to calculate other optical parameters.

4. RESULTS AND DISCUSSION

4.1. THE MAGNETOPHOTONIC CRYSTALS WITH MAGNETIC BRAGG MIRRORS

The magnetophotonic crystals with magnetic Bragg mirrors are composed of magnetic material sandwiched between two magnetic PCs constitutes of SiO_2 (D1) and $Bi:YIG$ (M). The $Bi:YIG$ (bismuth substituted yttrium iron garnet) is used as a magnetic material with high MO features. Bi:YIG has very strong spin-orbit coupling caused by high bismuth ion concentration which leads to high MO figure of merit at near-infrared communications wavelengths [38].

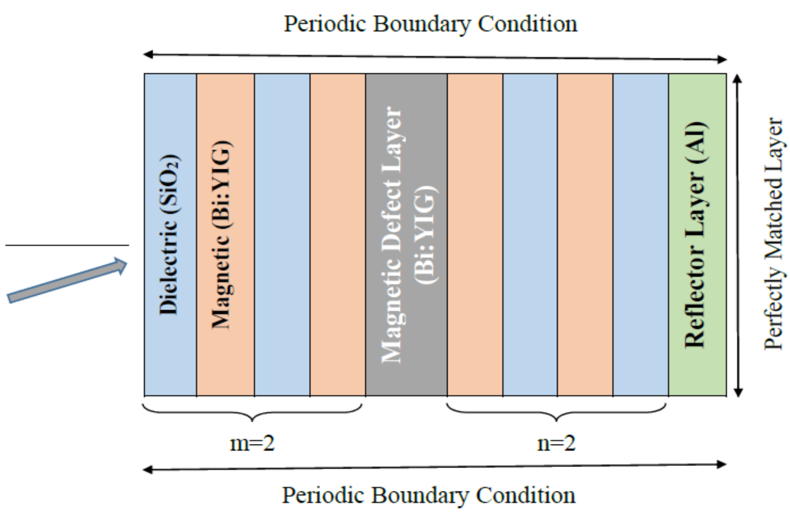

Fig. 1. Basic MPC structure composed of magnetic material (Bi:YIG) sandwiched between two magnetic PCs is shown (Dielectric 1= SiO_2 and Magnetic=Bi:YIG). The boundary conditions of FEM simulation are presented. m and n are repetition numbers of PCs at the right and left hand sides of the magnetic layer, respectively.

Magnetic garnets are attractive materials for MO studies because of their applications in non-reciprocal photonic devices, integrated MO tools, and spintronic phenomena [39-42]. The last layer is made of Al as reflector layer. The overview of these structures and boundary conditions of FEM simulation are shown in Fig. 1.

For the construction of MPCs, we used $Bi:YIG$ as the magnetic material that has diagonal and non-diagonal dielectric tensor elements $\varepsilon_{xx} = 4.75$ and $\varepsilon_{xy} = 2.69 \times 10^{-3}$ at $\lambda = 1.15\mu m$, respectively [43]. Moreover, we denoted SiO_2 and $Bi:YIG$ as D1 and M, respectively. The optical thickness of each dielectric and magnetic layers in magnetic Bragg mirrors was a quarter wavelength, but the magnetic defect layer had the optical thickness of the half wavelength. The refractive indices of dielectric materials and reflector layer are cited from [44]. At first, we considered the MPC in the form of MPC1: $(D1/M)^m(M)(M/D1)^n/Al$, with repetition numbers of m and n. Using TMM, we computed the reflection and Kerr rotation of MPC1 as a function of repetition numbers m and n. The results of these calculations, are shown in Fig. 2.

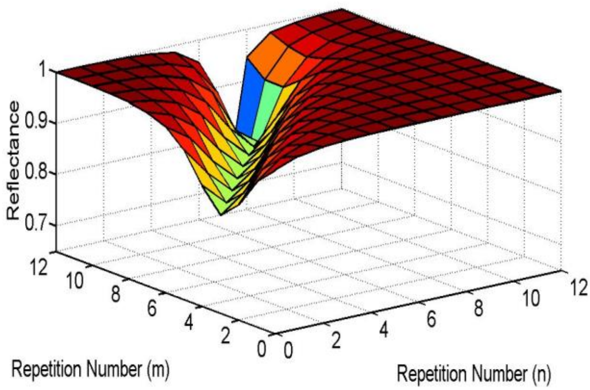

(a)

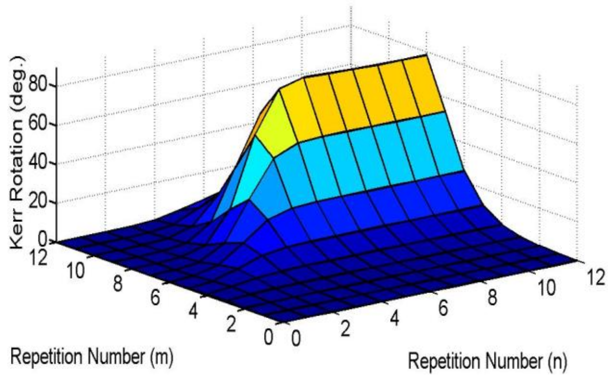

(b)

Fig. 2. (a) The reflectance and (b) the Kerr rotation angle of MPC1 versus the repetition numbers m and n.

Based on this figure, the MPC1 with m=8 and n=10 to n=12 has high reflectance and enhanced Kerr rotation simultaneously. For m=8 and n=11 and 12, the reflection and Kerr rotation angle is almost constant. Thus, we can introduce each of these cases as proper conditions for optical uses. As displayed in Fig. 3, for MPC1 with m=8 and n=12, the reflection is very close to 1 and Kerr rotation $\theta_K = 78^\circ$ at $\lambda = 1.15\mu m$.

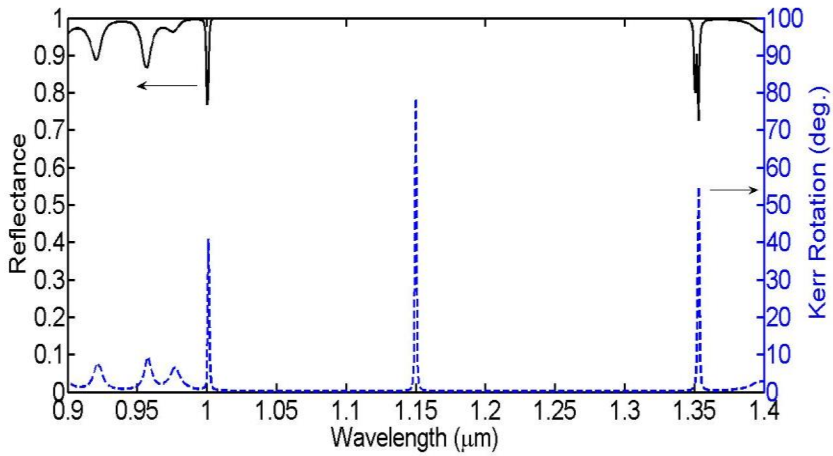

Fig. 3. The reflectance and Kerr rotation values based on the wavelength of incident wave for MPC1 with m=8 and n=12.

The Kerr rotation for wavelengths 1 μm and 1.36 μm is significantly increased, but the reflectance values are decreased. Therefore, the magneto-optical features at $\lambda = 1.15\mu m$ provide the best conditions for practical applications.

The distribution and magnitude of electric field in the length of MPC1 structure with m=8 and n=12 is computed with FEM simulation (Fig. 4). To our expectation, the intensity of the electric field within the magnetic defect layer has increased considerably and led to high MO responses through the multiple reflections of light within the cavity.

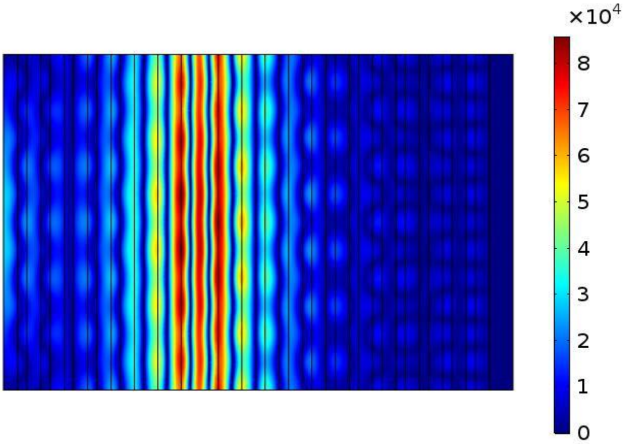

(a)

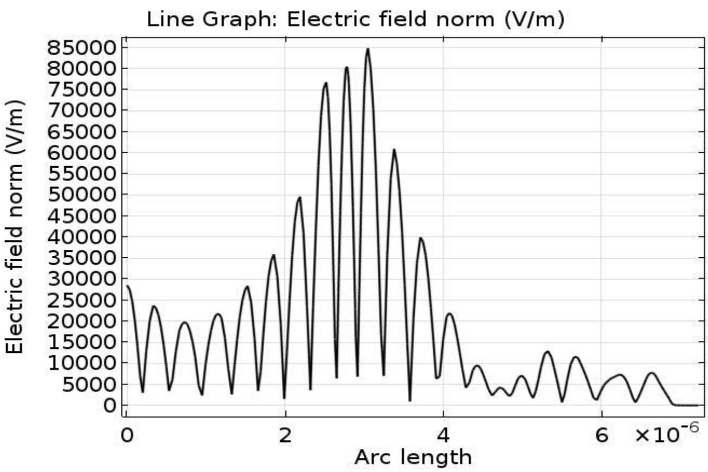

(b)

Fig. 4. a) The distribution and b) the magnitude of electric field in the length of MPC1 with m=8 and n=12. The electric field is localized in the vicinity and inside of the magnetic defect layer.

The magnitude of the electric field inside the magnetic defect layer is 3 times larger than that of the first layer of the structure. This is a good representation of the electric field localization in the magnetic cavity. This simulation is done for the initial wavelength equal to $\lambda = 1.15\mu m$.

Next, we calculated the reflectance and Kerr rotation of MPC1 versus the thickness of the magnetic defect layer. Similar to MPC1, the Kerr rotation angles are significantly increased at an optical thickness of $\frac{l\lambda}{2}$, where l is an integer number and $\lambda = 1.15\mu m$.

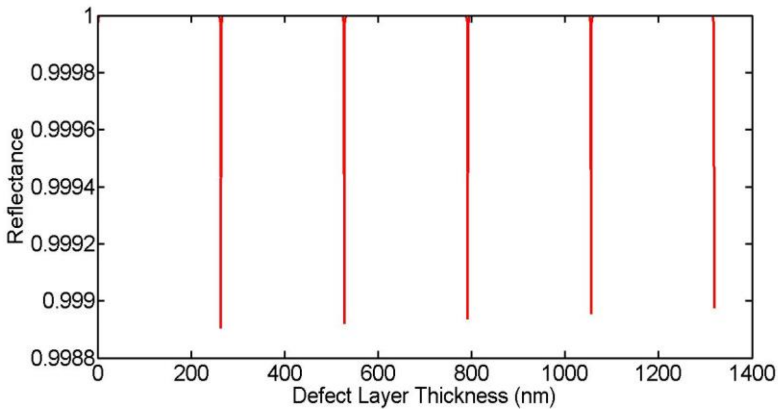

(a)

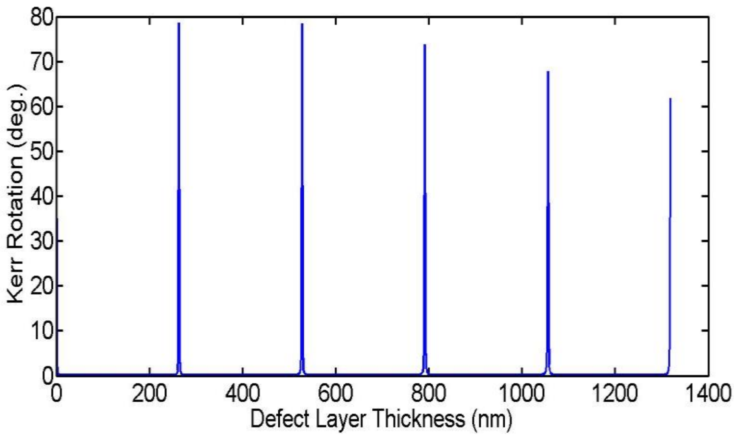

(b)

Fig. 5. (a) The reflectance and (b) the Kerr rotation for MPC1 with m=8 and n=12 versus the thickness of magnetic defect layer.

According to Fig. 5, the maximum values of the Kerr rotation angle are obtained for the magnetic cavities with optical thicknesses equal to $\frac{\lambda}{2}$ ($d_{Bi:YIG} = 263.8nm$) and λ ($d_{Bi:YIG} = 527.6nm$). The reflection values for these situations are almost equal and very close to 1. These conditions are suitable for designing MO tools. By increasing the $d_{Bi:YIG}$, the rotation angle peaks decreased slowly.

4.2. THE MAGNETOPHOTONIC CRYSTALS WITH DIELECTRIC BRAGG MIRRORS

In this section, we investigated the magnetophotonic structures with dielectric Bragg mirrors. In designing them, the $Bi:YIG$ magnetic layer has an optical thickness equal to the half wavelength sandwiched between two dielectric PCs composed of Si (D1) and SiO_2 (D2) with periodic configuration. The optical thickness of each dielectric layer is $\frac{\lambda}{4}$. The schematic of these magnetophotonic structures is illustrated in Fig. 6.

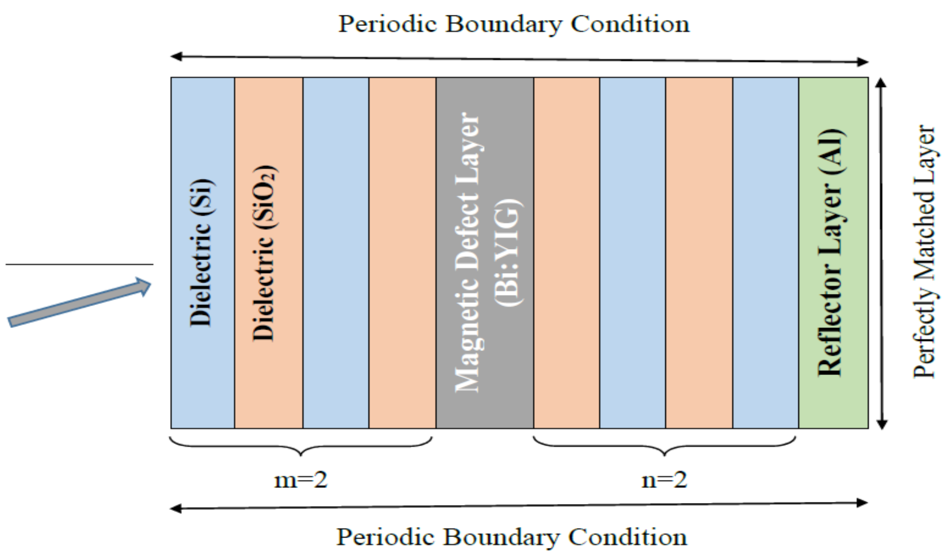

Fig. 6. Basic MPC structure composed of magnetic material (Bi:YIG) sandwiched between two dielectric PCs is shown (Dielectric 1= Si, Dielectric 2= SiO_2 and Magnetic= Bi:YIG). The boundary conditions of FEM simulation are presented. m and n are repetition numbers of PCs at the right and left hand sides of the magnetic layer, respectively.

We considered the MPC2:$(D1/D2)^m(M)(D2/D1)^n$ with repetition numbers of dielectric Bragg mirrors, m and n. By using TMM, the reflectance and Kerr rotation angle are calculated as a function of repetition numbers (Fig. 7).
The values of Kerr rotation are constant for m=3 and n=7 to n=12. With consideration of reflection values, the conditions mentioned above are suitable cases with simultaneous high reflectance and Kerr angle. Thus, we can introduce each of these cases as suitable configuration for designing of MO devices.
As exhibited in Fig. 8, we calculated the reflectance and Kerr rotation spectra for MPC2 structure with m=3 and n=10. These calculations are done in the wavelength region from 0.9 μm to 1.4 μm.

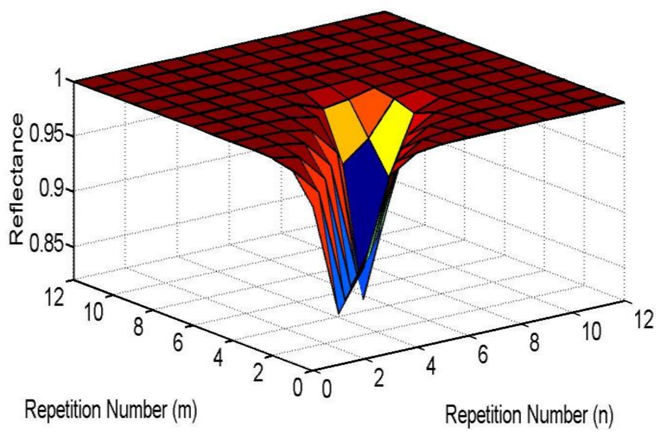

(a)

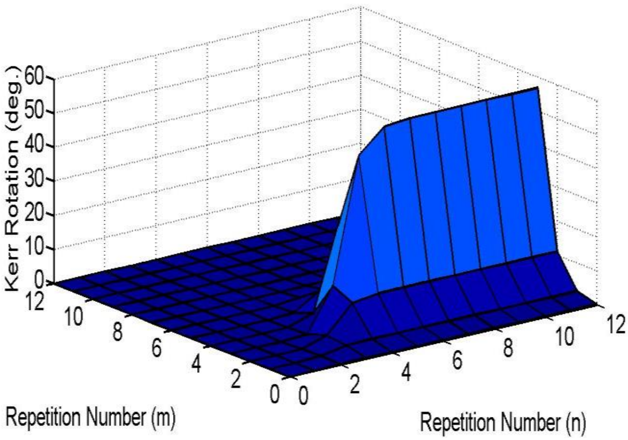

(b)

Fig. 7. (a) The reflectance and (b) the Kerr rotation angle of MPC2 versus the repetition numbers m and n.

For MPC2 with m=3 and n=10, the reflectance and the Kerr angle at $\lambda = 1.15 \mu m$ are $R = 99.9987\%$ and $\theta_k = 57^\circ$ respectively. We simulated the distribution of electric field in the length of this structure using FEM. As shown in Fig. 9, the electric field is localized inside the magnetic defect layer, which leads to enhancement of the Kerr rotation angle.

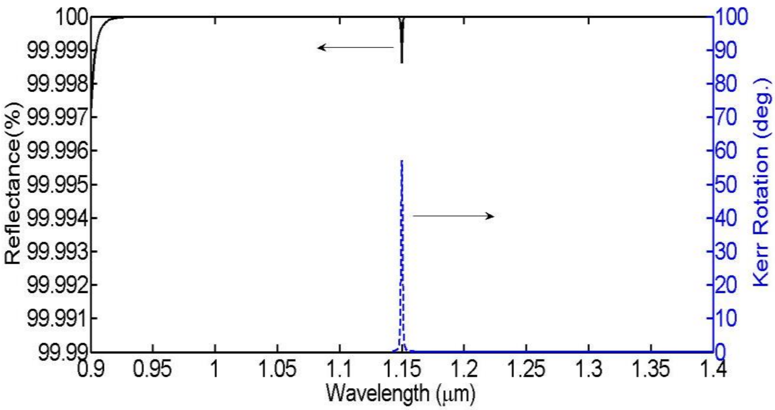

Fig. 8. The reflectance and Kerr rotation values based on the wavelength of incident wave for MPC2 with m=3 and n=10.

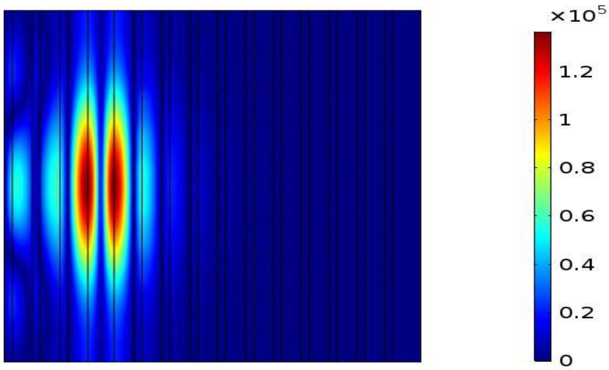

(a)

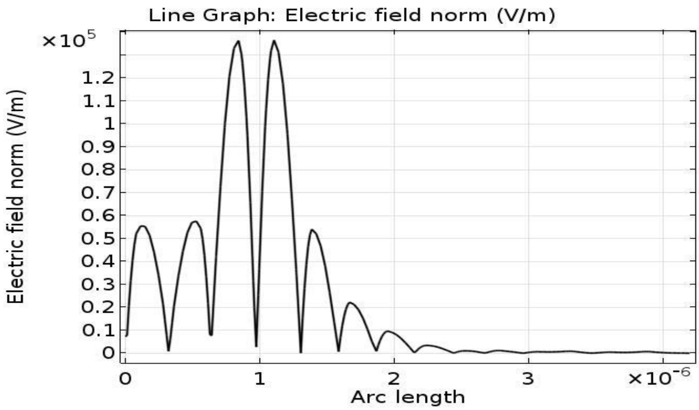

(b)

Fig. 9. a) The distribution and b) the magnitude of electric field in the length of MPC2 with m=3 and n=10. The electric field is localized inside the magnetic defect layer.

By increasing the optical path length and constructive interference between multiple reflections of light inside the magnetic defect layer, the MO responses of MPC2 structure are increased.

The thickness of the magnetic defect layer is an effective parameter on the MO features of magnetophotonic crystals. Therefore, we computed the reflectance and the Kerr rotation of MPC2 with m=3 and n=10 versus the thickness of the defect layer. The results of these calculations are exhibited in Fig. 10.

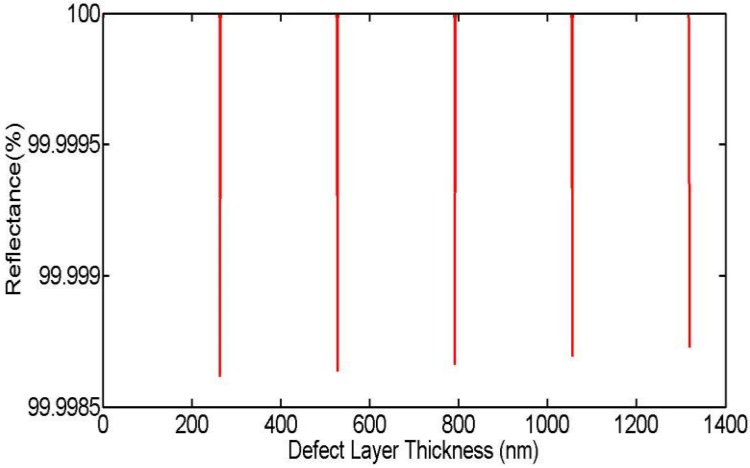

(a)

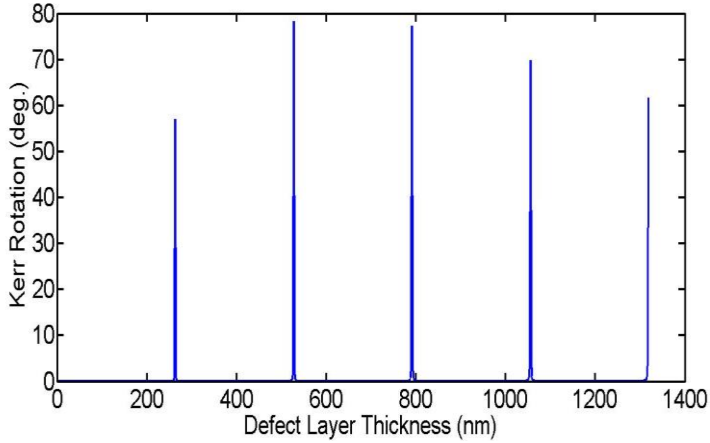

(b)

Fig. 10. (a) The reflectance and (b) the Kerr rotation for MPC2 with m=3 and n=10 versus the thickness of magnetic defect layer.

The reflectance and Kerr rotation are peaked at optical thicknesses equal to $\frac{l\lambda}{2}$ with $\lambda = 1.15\mu m$ where l is an integer number. The MPC2 structure with m=3 and n=10 and cavity thickness equal to 527.6 nm is the best case for a practical application. This structure provided $\theta_k = 78^\circ$ and a reflection very close to 1. The MO responses of the structure with an optical thickness of the cavity equal to $\frac{3\lambda}{2}$ partially differ from the prior case. Thus, these magnetophotonic crystals are good candidates to apply in MO devices.

5. CONCLUSION

Using the TMM, we investigated the MOKE in the one-dimensional magnetophotonic crystals with magnetic and dielectric Bragg mirrors. We have used of Bi:YIG as a magnetic material, because of high MO features and very strong spin-orbit coupling. The magnetic garnets such as Bi:YIG have high importance in MO devices designing due to spintronic phenomena such as spin Hall magneto-resistance and Seebeck effect.

In the most of the previous studies on magneto-optical Faraday and Kerr effects, the magnetophotonic structures have a spatial symmetry in which the magnetic defect layer is located in the middle of the structure and the periodic layers are located around it. Such a look at magnetophotonic crystals may ignore non-symmetric spatial structures with high magneto-optical responses. Therefore, the researches with regard to non-symmetric spatial structures can have a significant effect on the advancement of studies on optical devices to increase their optimality. In this paper, we considered the different repetition numbers, as two variables, for alternating layers around the magnetic defect layer. In this way, we simultaneously examined the magneto-optical responses of symmetric and non-symmetric spatial structures.

Considering the importance of light localization in the magnetic defect layer and the unique ability of the FEM to simulate the propagation of the fields in optical structures, we simulated the electric field distribution along the magnetophotonic structures and its magnitude using the FEM.

The repetition number of Bragg mirrors and thickness of defect layer are effective parameters in enhancing the MO responses that were studied in this paper. By adjusting the repetition numbers of the Bragg mirrors, we obtained structures with high reflectance and large Kerr rotation simultaneously, which are suitable for designing MO devices.

For magnetophotonic crystals with magnetic Bragg mirrors, the cases with m=8 and n=11 and 12 provide an optimal condition with high Kerr rotation equal to 78˚ and reflection very close to 1. For these structures, the light is intensively localized at the magnetic defect layer. The multiple reflections at the defect layer and increasing the length of the light path at the defect layer led to high MO responses. The reflectance and the Kerr rotation angle are maximized at the cases with an optical thickness of cavity equal to $\frac{l\lambda}{2}$. For magnetophotonic crystals with magnetic Bragg mirrors, by increasing the cavity thicknesses, the Kerr angles are decreased. The magnetophotonic structures with dielectric Bragg mirrors have large Kerr rotation and reflectance. These structures with an optical thickness of cavity equal to λ and $\frac{3\lambda}{2}$ are suitable structures to apply in MO tools. For these cases, the Kerr angles are maximized such that they reach 78˚. The reflections and Kerr rotations for these cases are approximately equal. For the structures studied in this research, the localization of light inside the magnetic defect layer has led to an increase in MO properties of magnetophotonic crystals.

REFERENCES

[1] A. A. Fedyanin, O. A. Aktsipetrov, D. Kobayashi, K. Nishimura, H. Uchida and M. Inoue, *Enhanced Faraday and nonlinear magneto-optical Kerr effects in magnetophotonic crystals*, J. Magn. Magn. Mater. 282 (2004) 256-259.

[2] K. Sakoda, *Optical Properties of Photonic Crystals*, 2nd Edition, Springer. New York, USA, 2004.

[3] J. D. Joannopoulos, S. G. Johnson, J. N. Winn and R. D. Meade, *Photonic Crystals:Molding the Flow of Light*, Princeton University Press, 2nd edition. New Jersey, USA, 2008.

[4] Z. Zare and A. Gharaati, *Investigation of thermal tunable nano metallic photonic crystal filter with mirror symmetry*, JOPN. 3 (3) (2018) 27-36.

[5] E. Yablonovitch, *Inhibited spontaneous emission in solid-state physics and electronics*, Phys. Rev. Lett. 58 (20) (1987) 2059-2062.

[6] S. John, *Strong localization of photons in certain disordered dielectric superlattices*, Phys. Rev. Lett. 58 (23) (1987) 2486-2489.

[7] J. C. Knight, J. Broeng, T. A. Birks and P. St. J. Russell, *Photonic Band Gap Guidance in Optical Fibers*, Science. 282 (5393) (1998) 1476-1478.

[8] Z. Wu, K. Xie and H. Yang, *Band gap properties of two-dimensional photonic crystals with rhombic lattice*, Optik. 123 (6) (2012) 534-536.

[9] Y. A. Vlasov, X. Bo, J. C. Sturm and D. J. Norris, *On-chip natural assembly of silicon photonic bandgap crystals*. Nature. 414 (2001) 289-293.

[10] M. W. Haakestad, T. T. Alkeskjold, M. D. Nielsen, L. Scolari, J. Rishede, H. E. Engan and A. Bjarklev, *Electrically tunable photonic bandgap guidance in a liquid-crystal filled photonic crystal fiber*, IEEE Photon. Tech. Lett. 17 (4) (2005) 819-821.

[11] O. Painter, R. K. Lee, A. Scherer, A. Yariv, J. D. O'Brien, P. D. Dapkus

and I. Kim, *Two-Dimensional Photonic Band-Gap Defect Mode Laser*, Science. 284 (5421) (1999) 1819-1821.

[12] Y. Kubota, M. Taguchi, H. Akai, Sh. Yamamoto, T. Someya, Y. Hirata, K. Takubo, M. Araki, M. Fujisawa, K. Yamamoto, Y. Yokoyama, S. Yamamoto, M. Tsunoda, H. Wadati, S. Shin and I. Matsuda, *L-edge resonant magneto-optical Kerr effect of a buried Fe nanofilm*, Phys. Rev. B. 96 (13) (2017) 134432.

[13] T. Haider, *A Review of Magneto-Optic Effects and Its Application*, Int, J. Electromag, Appl. 7 (2017) 17-24.

[14] R. Abdi-Ghaleh and A. Namdar, *Circular polarization bandpass filters based on one-dimensional magnetophotonic crystals*, J. Mod. Opt. 60 (19) (2013) 1619-1626.

[15] M. Inoue, M. Levy and A. V. Baryshev, *Magnetophotonics: From theory to applications*, Springer, Berlin, Germany, 2013.

[16] V. I. Belotelov and A. K. Zvezdin, *Magneto-optical properties of photonic crystals*, J. Opt. Soc. Amer. 22 (1) (2005) 286-292.

[17] R. Abdi-Ghaleh and M. Asad, *Design of one-dimensional magnetophotonic crystals operating at visible wavelengths*, Eur. Phys. J. D. 69 (13) (2015) 1-7.

[18] A. K. Zvezdin and V. I. Belotelov, *Magnetooptical properties of two dimensional photonic crystals*, Eur. Phys. J. B. 37 (4) (2004) 479-487.

[19] W. K. Tse and A. H. MacDonald, *Giant Magneto-optical Kerr Effect and Universal Faraday Effect in Thin-Film Topological Insulators*, Phys. Rev. Lett. 105 (5) (2010) 057401.

[20] G. M. Choi, *Magneto-Optical Kerr Effect Driven by Spin Accumulation on Cu, Au, and Pt*, Appl. Sci. 8 (8) (2018) 1378.

[21] S. Kumari and S. Chakraborty, *Study of different magneto-optic materials for current sensing applications*, J. Sens. Sens. Syst. 7 (2018) 421-431.

[22] M. Inoue, K. I. Arai, T. Fujii and M. Abe, O*ne-dimensional magnetophotonic crystals*, J. App. Phys. 85 (8) (1999) 5768-5770.

[23] K. J. Vahala, *Optical microcavities*, Nature. 424 (2003) 839-846.

[24] N. E. Khokhlov, A. R. Prokopov, A. N. Shaposhnikov, V. N. Berzhansky, M. A. Kozhaev, S. N. Andreev, A. P. Ravishankar, V. G. Achanta, D. A. Bykov, A. K. Zvezdin and V. I. Belotelov, *Photonic crystals with*

plasmonic patterns: novel type of the heterostructures for enhanced magneto-optical activity, J. Phys. D: Appl. Phys. 48 (9) (2015).

[25] A. L. Chekhov, V. L. Krutyanskiy, A. N. Shaimanov, A. I. Stognij and T. V. Murzina, *Wide tunability of magnetoplasmonic crystals due to excitation of multiple waveguide and plasmon modes*, Opt. Express. 22 (15) (2014) 17762-17768.

[26] M. Pohl, L. E. Kreilkamp, V. I. Belotelov, I. A. Akimov, A. N. Kalish, N. E. Khokhlov, V. J. Yallapragada, A. V. Gopal, M. NurE-Alam and M. Vasiliev, *Tuning of the transverse magneto-optical Kerr effect in magneto-plasmonic crystals*, New J. Phys. 15 (2013).

[27] C. Y. You and S. C. Shin, *Generalized analytic formulae for magneto-optical Kerr effects*, J. App. Phys. 84 (1) (1998) 541-546.

[28] I. Abdulhalim, *Analytic propagation matrix method for anisotropic magneto-optic layered media*, J. Opt. A: Pure. Appl. Opt. 2 (6) (2000) 557-564.

[29] A. K. Zvezdin and V. A. Kotov, *Modern magnetooptics and magnetooptical materials*, IOP Publishing Ltd, Bristol and Philadelphia, 1997.

[30] M. Mansuripur, *The physical principles of magneto-optical recording*, Cambridge University Press, New York, USA, 1995.

[31] Y. A. Uspenskii, E. T. Kulatov and S. V. Halilov, *Effect of anisotropy on magneto-optical properties of uniaxial crystals: Application to CrO2*, Phys. Rev. B. 54 (1) (1996) 474-481.

[32] T. Kaihara, T. Ando, H. Shimizu, V. Zayets, H. Saito, K. Ando and S. Yuasa, *Enhancement of magneto-optical Kerr effect by surface plasmons in trilayer structure consisting of double-layer dielectrics and ferromagnetic metal*, OSA. Opt. Express. 23 (9) (2015) 11537-11555.

[33] C. Dehesa-Martinez, L. Blanko-Gutierrez, M. Velez, J. Diaz, L. M. Alvarez-Prado and J. M. Alameda, *Magneto-optical transverse Kerr effect in multilayers*, Phys. Rev. B. 64 (2) (2001) 024417.

[34] J. Zak, E. R. Moog, C. Liu and S. D. Bader, *Fundamental magnetooptics*, J. Appl. Phys. 68 (8) (1990).

[35] M. Zamani, M. Ghanaatshoar and H. Alisafaee, *Compact one-dimensional magnetophotonic crystals with simultaneous large Faraday rotation and high transmittance*, J. Mod. Opt. 59 (2) (2012) 126-130.

[36] W. Reim and D. Weller, *Kerr rotation enhancement in metallic bilayer thin films for magnetooptical recording*, App. Phys. Lett. 53 (24) (1988) 2453-2457.

[37] J. Bastos and N. Sadowski , *Electromagnetic Modeling by Finite Element Method*, CRC Press, Boca Raton, USA, 2003.

[38] E. Jesenska, T. Yoshida, K. Shinozaki, T. Ishibashi, L. Beran, M. Zahradnik, R. Antos, M. Kučera and M. Veis, *Optical and magneto-optical properties of Bi substituted yttrium iron garnets prepared by metal organic decomposition*, Opt. Soc. Amer. 6 (6) (2016) 261138.

[39] S. Yamamoto and I. Matsuda, *Measurement of the Resonant Magneto-Optical Kerr Effect Using a Free Electron Laser*, Appl. Sci. 7 (7) (2017) 662-1-23.

[40] E. Lage, L. Beran, A. U. Quindeau, L. Ohnoutek, M. Kucera, R. Antos, S. R. Sani, G. F. Dionne, M. Veis and C. A. Ross, *Temperature-dependent Faraday rotation and magnetization reorientation in cerium-substituted yttrium iron garnet thin films*, APL. MATERIALS. 5 (2017) 036104-1-7.

[41] M. Barthelemy, M. Vomir, M. Sanches Piaia, H. Vonesch, P. Molho, B. Barbara, and J. Y. Bigot, *Magneto-optical four-wave mixing transients in garnets*, Opt. Soc. Amer: Optica. 4 (1) (2017) 60-63.

[42] C. Tang, M. Aldosary, Z. Jiang, H. Chang, B. Madon, K. Chan, M. Wu, J. E. Garay and J. Shi, *Exquisite growth control and magnetic properties of yttrium iron garnet thin films*, Appl. Phys. Lett. 108 (10) (2016) 102403-1-17.

[43] M. Levy, H. C. Yang, M. J. Steel and J. Fujita, *Flat-Top Response in One-Dimensional Magnetic Photonic Bandgap Structures With Faraday Rotation Enhancement*, J. Lightwave. Technol. 19 (12) (2001) 1964-1969.

[44] http://refractiveindex.info, Accessed on: 2018/10/25.